

Regional Differences in the Carbon Source-Sink Potential of Natural Vegetation in the U.S.A.

DOMINIQUE BACHELET

Dept of Bioengineering
Oregon State University,
Corvallis, Oregon 97331, USA

RONALD P. NEILSON

JAMES M. LENIHAN

RAYMOND J. DRAPEK

USDA Forest Service Pacific Northwest Research Station
Forestry Sciences Laboratory
3200 Jefferson Way SW
Corvallis, Oregon 97331, USA

ABSTRACT / We simulated the variability in natural ecosystem carbon storage under historical conditions (1895–1994) in six regions of the conterminous USA as delineated for the US-GCRP National Assessment (2001). The largest simulated variations in carbon fluxes occurred in the Midwest, where large fire events (1937, 1988) decreased vegetation biomass and soil carbon pools. The Southeast showed decadal-type

trends and alternated between a carbon source (1920s, 1940s, 1970s) and a sink (1910s, 1930s, 1950s) in response to climate variations. The drought of the 1930s was most obvious in the creation of a large carbon source in the Midwest and the Great Plains, depleting soil carbon reserves. The Northeast shows the smallest amplitudes in the variation of its carbon stocks. Western regions release large annual carbon fluxes from their naturally fire-prone grassland- and shrubland-dominated areas, which respond quickly to chronic fire disturbance, thus reducing temporal variations in carbon stocks. However, their carbon dynamics reflect the impacts of prolonged drought periods as well as regional increases in rainfall from ocean-atmosphere climate regime shifts, most evident in the 1970s. Projections into the future by using the warm CGCM1 climate scenario show the Northeast becoming mostly a carbon source, the Southeast becoming the largest carbon source in the 21st century, and the two western-most regions becoming carbon sinks in the second half of the 21st century. Similar if more moderate trends are observed by using the more moderately warm HADCM2SUL scenario.

The size of terrestrial carbon sinks and the interaction of these sinks with anthropogenic emissions of CO₂ have proved controversial. The existence and the size of a sink in the continental USA is difficult to estimate. Attempts to define sinks at the regional level are full of uncertainties and contradictions. Using inverse-modeling techniques based on atmospheric and oceanic data and models, Fan and others (1998) calculated a continental United States carbon sink for the early 1990s of 0.81 Pg C y⁻¹ (1.7 Pg C y⁻¹ for the entire North American continent), whereas Bousquet and others (2000), using similar techniques, estimated the sink to be as much as 2 Pg C y⁻¹ during the early 1990s for the entire North American continent. Observations of atmospheric gas concentrations and atmospheric transport models have also suggested a Northern Hemisphere mid-latitude terrestrial sink of 1–3 Pg C y⁻¹. On the other hand, Schimel and others (2000) and Potter and Klooster (1999), using biogeochemical models, published values around 0.2 Pg C y⁻¹. Similarly, forest inventory data (Birdsey and others 1993, Birdsey and

Heath 1995, Turner and others 1995, Brown and Schroeder 1999) have generated carbon sequestration rates by North American forest ecosystems between 0.08 and 0.28 Pg C y⁻¹. By including anthropogenic effects, such as changes in agricultural soils due to management practices (e.g. conservation tillage), woody encroachment in the western U.S., and fire suppression, Houghton and others (1999) estimated the upper limit for carbon sequestration in the United States at 0.35 Pg C y⁻¹.

Most of the uncertainty among these various estimates arises from the lack of integration of information rather than the lack of knowledge (Falkowski and others 2000). The combined effects of increasing CO₂ concentrations (Keeling and others 1989), warmer night-time temperatures (Easterling and others 1997), climatic fluctuations (Easterling and others 2000), and anthropogenic impacts such as pollution, land conversion, water diversion combine to complicate the issue. Attempts to resolve this situation are continuing. For example, Pacala and others (2001) summarized and reconciled the results from all these studies and came up with a carbon sink estimate of 0.30 to 0.58 Pg C y⁻¹ for the conterminous USA.

Published online May 20, 2004.

Reports on carbon pools at global or continental scales do not reveal regional differences that are important to land-use managers and economists. We present results from the Vegetation Ecosystem Modeling Analysis Project (VEMAP) for each of the six regions in the U.S. Global Climate Change National Assessment Report (NAST 2000). We report only on areas with 'natural' vegetation. Although we masked out cultivated areas, it is important to note that we do not incorporate any past human influences on the 'natural' vegetation that we simulate, such as forest harvest and fire suppression practices. At least some of the present carbon sink in the U.S. is being attributed to the recovery of forests from widespread harvest over the past two centuries, abandonment of agricultural lands, and the suppression of fires in the West, allowing the expansion of woody vegetation (Pacala and others 2001). Nevertheless, even though virtually all ecosystems have been influenced by humans, ecosystems must still function within the constraints of the natural climate and its interannual, interdecadal, and regional variability.

We analyzed the regional and interdecadal variability of carbon source-sink dynamics over the conterminous U.S. for the past 100 years, using the MC1 dynamic vegetation model (DVM) to further understand the contributions of regional and temporal variation in climate to the overall U.S. carbon source-sink debate. In addition, we used two future climate scenarios to project what each region might face in the 21st century: a moderately warm scenario from the Hadley Climate Center and a much warmer scenario from the Canadian Climate Center. Both include sulfate aerosols and assume a gradual CO₂ increase. Rather than predicting accurate levels of carbon sequestration or losses, this study highlights the areas that are most sensitive to small changes in predicted rainfall and temperature. It offers reasonable outcomes to projected changes in climate from current knowledge and assumptions, and offers options to be considered by land-use managers of forest and rangelands.

Methods

Dynamic Vegetation Model MC1

MC1 (Daly and others 2000, Bachelet and others 2001a) is a dynamic vegetation model (DVM) that simulates lifeform mixtures and vegetation types; fluxes of carbon, nitrogen, and water; and fire disturbance (Lenihan and others 1998). MC1 is routinely implemented (Daly and others 2000, Bachelet and others 2000, 2001b, Aber and others 2001) on spatial data grids of varying resolution (i.e., grid cell sizes ranging

from 4 km² to 0.5 degree latitude/longitude) where the model is run separately for each grid cell (i.e., there is no exchange of information across cells). The model reads climate data at a monthly time-step to run interacting modules that simulate biogeography, biogeochemistry, and fire disturbance.

The biogeography module simulates the potential lifeform mixture of evergreen needleleaf, evergreen broadleaf, and deciduous broadleaf trees, and C3 and C4 grasses. The tree lifeform mixture is determined at each annual time-step by locating the grid cell on a two-dimensional gradient of annual minimum temperature and growing season precipitation. Lifeform dominance is arrayed along the minimum temperature gradient from evergreen needleleaf dominance at relatively low temperatures, to deciduous broadleaf dominance at intermediate temperatures, to broadleaf evergreen dominance at relatively high temperatures. Growing season precipitation (GSP) is used to modulate the relative dominance of deciduous broadleaved trees, which is gradually reduced to zero towards low values of GSP. Mixtures of C3 and C4 grasses are determined by calculating their relative potential productivity during the summer months as a function of soil temperature. The tree and grass lifeform mixtures together with leaf biomass simulated by the biogeochemistry module are used in a set of rules to determine which of 22 possible potential vegetation types occurs at a grid cell each year. The MC1 biogeography rules were developed by using MAPSS (Neilson 1995) as a template.

The biogeochemistry module is a modified version of the CENTURY model (Parton and others 1987, 1994). It simulates plant productivity, organic matter decomposition, and water and nutrient cycling. Plant productivity is constrained by temperature, effective moisture (i.e., a function of soil moisture and potential evapotranspiration), and nutrient availability. The simulated effect of increasing atmospheric CO₂ is to increase maximum potential production and to decrease transpiration (thus reducing the constraint of effective moisture on productivity). Trees compete with grasses for soil moisture, light, and nutrients. Competition for water is structured by root depth. Trees and grasses compete for soil moisture in the upper soil layers where both lifeforms are rooted, while the deeper-rooted trees have sole access to moisture in deeper layers. Grass productivity is constrained by light availability in the understory, which is reduced as a function of tree leaf biomass. Parameterization of the tree and grass growth processes in the model is based on the current lifeform mixture, which is updated annually by the biogeography module. For example, an increase in

annual minimum temperature that shifts the dominance of evergreen needle-leaved trees to co-dominance with evergreen broadleaved trees will trigger an adjustment of tree growth parameters (e.g., the optimum growth temperature) that will, in turn, produce a different tree growth rate.

The MC1 fire module (Lenihan and others 1998) simulates the occurrence, behavior and effects of fire. The module consists of several mechanistic fire behavior and effect functions (Rothermel 1972, Peterson and Ryan 1986, van Wagner 1993, Keane and others 1997) embedded in a structure that provides two-way interactions with the biogeography and biogeochemistry modules. Thresholds of fire spread, fine fuel flammability, and coarse woody fuel moisture trigger a fire event given a constraint of just one fire event per year. The thresholds were calibrated to limit the occurrence of simulated fires to only the most extreme events. Large and severe fires account for a very large fraction of the annual area burned historically in the western U.S. (Strauss and others 1989). These events are also likely to be least constrained by heterogeneities in topography and by fuel moisture and loading that are poorly represented by relatively coarse-scale input data grids (Turner and Romme 1994). The direct effect of fire in the model is the consumption and mortality of dead and live vegetation carbon that is removed from (or transferred to) the appropriate carbon pools in the biogeochemistry module. The fraction of the cell burned depends on the simulated rate of fire spread and the time since the last fire event relative to the current fire return interval simulated for the cell. Higher rates of spread and longer intervals between fires generally produce more extensive fire events in the model. Live carbon mortality and consumption within the area burned are functions of fire intensity and tree canopy structure (i.e., crown height, crown length, and bark thickness). Dead biomass consumption is simulated with functions of fire intensity and fuel moisture that are fuel-class specific.

Climate Data

The climate data consist of monthly time-series for all the necessary variables (i.e., precipitation, minimum and maximum temperature, and vapor pressure deficit) distributed on a 0.5 degree latitude/longitude (ca. 50 km \times 50 km resolution) data grid for the conterminous United States (Kittel and others, 2000, 2003). Spatially distributed monthly time-series data for historical (1895–1993) precipitation, temperature, and vapor pressure were generated from observed station data interpolated to the data grid by the PRISM model (Daly and others, personal communication). Vapor pressure

deficit was estimated by subtracting vapor pressure from the saturated vapor pressure estimated from the monthly minimum temperature. The data were provided by the Data Analysis Group from the National Center for Atmospheric Research (NCAR), Boulder, Colorado (Kittel and others, 2000, 2003).

Spatially distributed future climate time-series (1994–2100) were constructed by using coarse-scale monthly output generated by two general circulation models (GCMs): a moderately warm scenario from the Hadley Climate Center model (HADCM2SUL) with up to a 2.8°C increase in average annual U.S. temperature in 2100 (Johns and others, 1997; Mitchell and Johns, 1997), and a warmer scenario from the Canadian Climate Center model (CGCM1) with up to a 5.8°C increase in average annual U.S. temperature in 2100 (Boer and others, 1999a, b; Flato and others, 1999). Both GCMs include the influence of dynamic oceans and aerosol forcing on the atmosphere. Both GCMs use IPCC projections of gradual (1% y^{-1}) greenhouse gas concentrations (IS92a) (Kattenberg and others 1996) in the future such that the CO₂ atmospheric concentration reaches 712 ppm in year 2100. These scenarios were also provided by NCAR.

Protocol to Run MC1

Equilibrium mode: initialization phase. The MAPSS equilibrium biogeography model (Neilson 1995) is first run (stand-alone mode) with mean 1895–1994 monthly climate data and soil information to produce an initial potential vegetation map. The MC1 biogeochemistry module is then initialized with this vegetation map and run with the same mean climate to calculate corresponding initial carbon and nitrogen pools. The run terminates when the slow soil organic matter pool reaches steady state, which may require up to 3000 simulation years for certain vegetation types (Daly and others 2000). This phase corresponds to the initialization of all MC1 variables. Because MC1's fire module cannot be run meaningfully on a mean climate, fire frequency is prescribed for each vegetation type in this equilibrium phase.

Transient mode with spin-up phase. Once the slow-turnover soil carbon pools have equilibrated, MC1 is run in transient mode by using a climate time series. This time series is created by linking the spin-up climate time series (100 years) provided by NCAR and the transient climate of interest (historical followed by future, 200 years total). The MC1 fire module is used only in transient mode and requires the spin-up phase to attain a spatially variable fire frequency and an overall dynamic equilibrium in net ecosystem carbon exchange with variable ecosystem age classes.

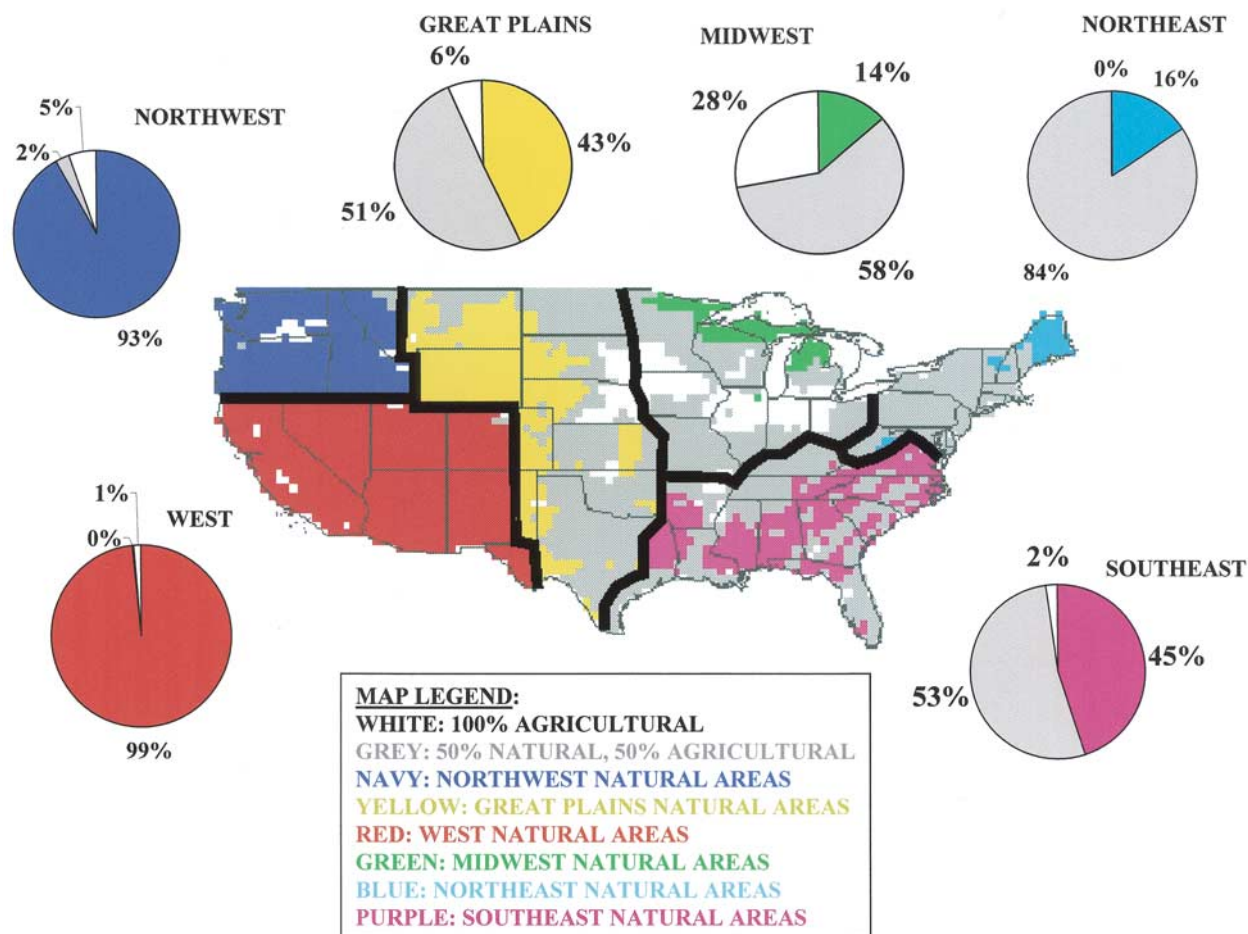


Figure 1. Map of the U.S. GCRP regions (NAST 2000) with the VEMAP agricultural mask overlaid. White represent 100% agricultural land-use, grey areas represent mixed (50% agricultural-50% natural) land-use. Each region natural area is represented by a different color: navy for the Northwest, green for the Midwest, blue for the Northeast, red for the West, yellow for the Great Plains, and purple for the Southeast. Pie charts show the fraction of each region that is natural, agricultural (white), or mixed land-use (grey). The model was not run for agricultural areas.

Model Output

The data presented in this paper correspond to the cumulative change in total ecosystem and soil carbon since 1895. These changes were calculated as the difference between the carbon pool at year y and the carbon pool at year 1895. We assumed that the carbon pools in 1895 just following the spinup period corresponded to a reasonably stable historical average.

We also calculated 10-year running averages for the annual changes in live-plant carbon and soil carbon (including litter). The annual change in a carbon pool was calculated as the difference between the pool size at year y and that at year $y-1$. We chose a ten-year running average to smooth out the year-to-year variability and better display decadal trends since carbon budgets are often reported as decadal averages in the recent liter-

ature. The change in total ecosystem carbon pool, also called net biological production, is also presented as a decadal average. It includes losses by fire.

“Biomass consumed by fire” represents carbon released to the atmosphere, but does not include the biomass that is killed without being consumed by fire. Biomass killed but not consumed by fires is added to the litter pools, from which it is released slowly through decomposition. This is an important point as other DGVMs do not include the inputs of dead biomass to soil carbon pools after a fire (Bachelet and others, 2003).

The model was run only for the area of natural vegetation in the conterminous United States. An agricultural mask (Schimel and others 2000) was overlaid on the regional map of the U.S. (Figure 1), including

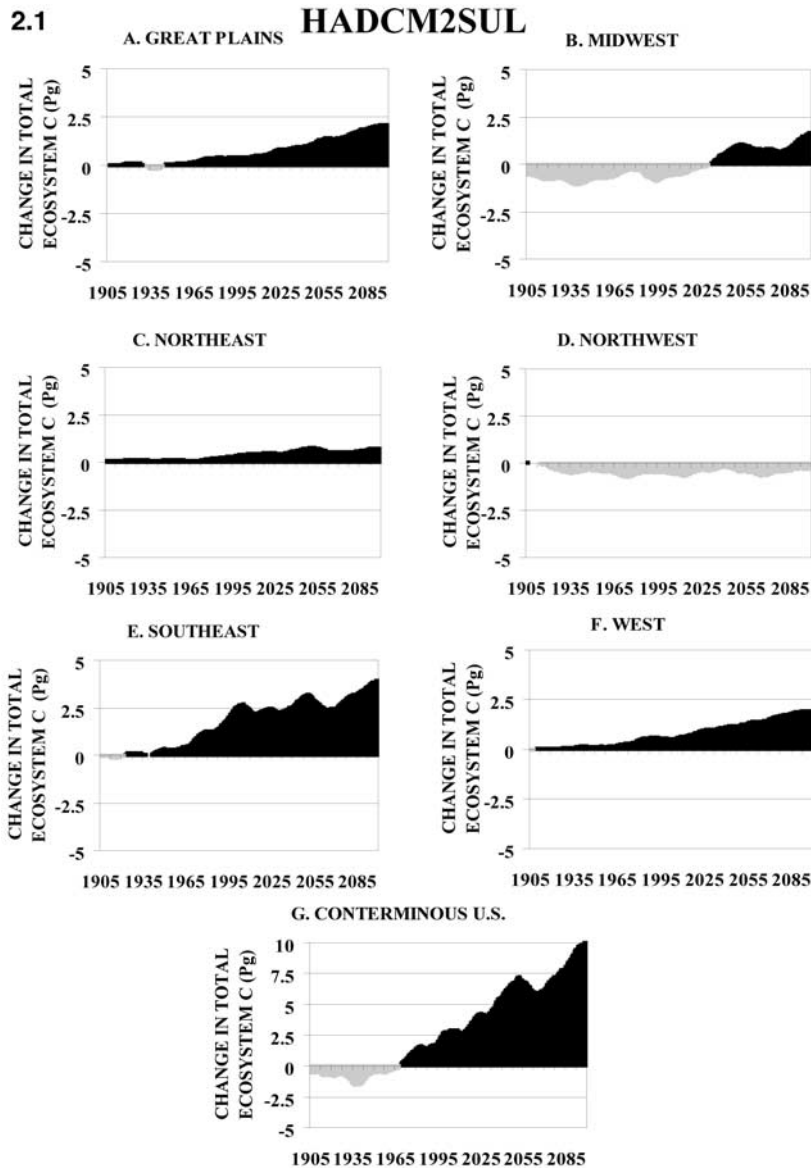


Figure 2. Annual change in total ecosystem carbon (10-year average) relative to the 1895 level for the 6 U.S. GCRP regions as simulated by MC1 from 1895 to 1993 and using (1) HADCM2SUL and (2) CGCM1 future climate change scenarios from 1994 to 2100.

three categories of land: 100% agricultural, 50% agricultural and 50% natural vegetation, 100% natural vegetation. The model was run on all the grid cells that supported the natural vegetation and on half of each grid cell that was described as mixed agricultural and natural vegetation. The model was not run for agricultural areas, since the vegetation types simulated by MC1 do not include crop species and since a time series of agricultural inputs (fertilizer levels and irrigation schedules) for historical and future periods would have been difficult, if possible at all, to obtain for each grid cell. The delineation of the regions (Figure 1) was defined in the U.S. Global Climate Change Program National Assessment Report (2000).

Results

Changes in Carbon Pool Sizes during the Historical Period from the 1895 Levels

When one compares the size of the total ecosystem carbon pool to the 1895 value, regional differences appear (Figure 2): the West, the Great Plains, the Northeast, and the Southeast regions show an increase in total carbon from the 1895 level between the beginning and the end of the 20th century. In the Great Plains region, the model simulates a decrease in total carbon following the drought of the 1930s. The model simulates both the Midwest (up to 1 Pg C) and the Northwest (up to 0.8 Pg C) regions as losing carbon in

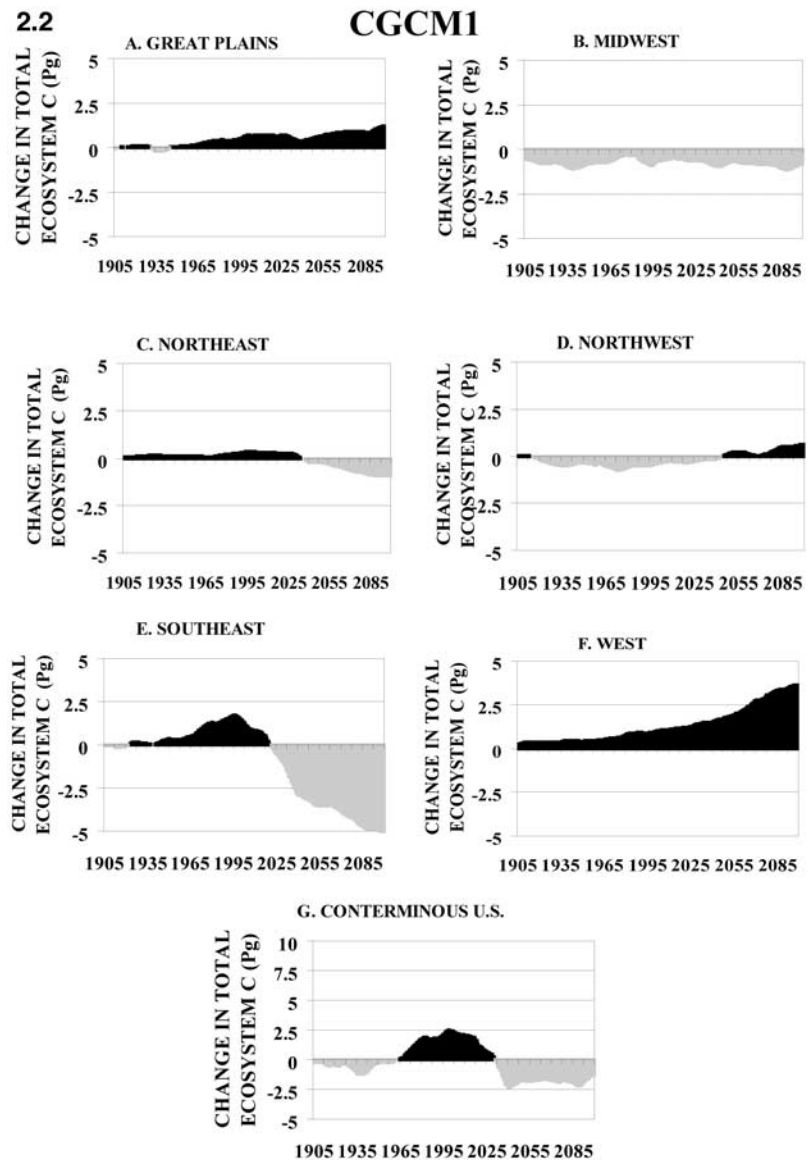


Figure 2. Continued.

the 20th century compared with the 1895 levels. Averaged over the entire country, the total carbon stocks evolve from losing carbon (up to -2 Pg C) in the 1st half of the 20th century to gaining carbon (up to 2 Pg C) in the 2nd half of the century (Fig 2.1 and 2.2G).

Changes in soil carbon levels since 1895 follow similar patterns (Figure 3). The Midwest and the Northwest exhibit the largest declines in soil carbon (about -0.5 Pg C). In the Southeast, the model simulates declines in soil carbon for most of the 20th century (Figure 3E) even though total system carbon increases steadily (Figure 2.1E). Soil carbon increases only from the 1970s until the end of the 20th century. For the country as a whole, soil carbon decreases from 1895

until the mid-1970s (up to -1 Pg C), but increases thereafter (Fig 3.1 and 3.2G).

Future Climatic Trends (1994–2100)

We did not simulate the climate, but feel it is important to document the climatic trends that drove our model to simulate vegetation response to future climate. Both future climate scenarios show an increase in annual temperature relative to the historical base period (1895–1993), but the increase is greater for the CGCM1 scenario (Figure 4 A and B). Both scenarios simulate a nearly 22% increase in precipitation over the conterminous U.S. by the end of the 21st century, although CGCM1 shows a decrease of about 4% by the

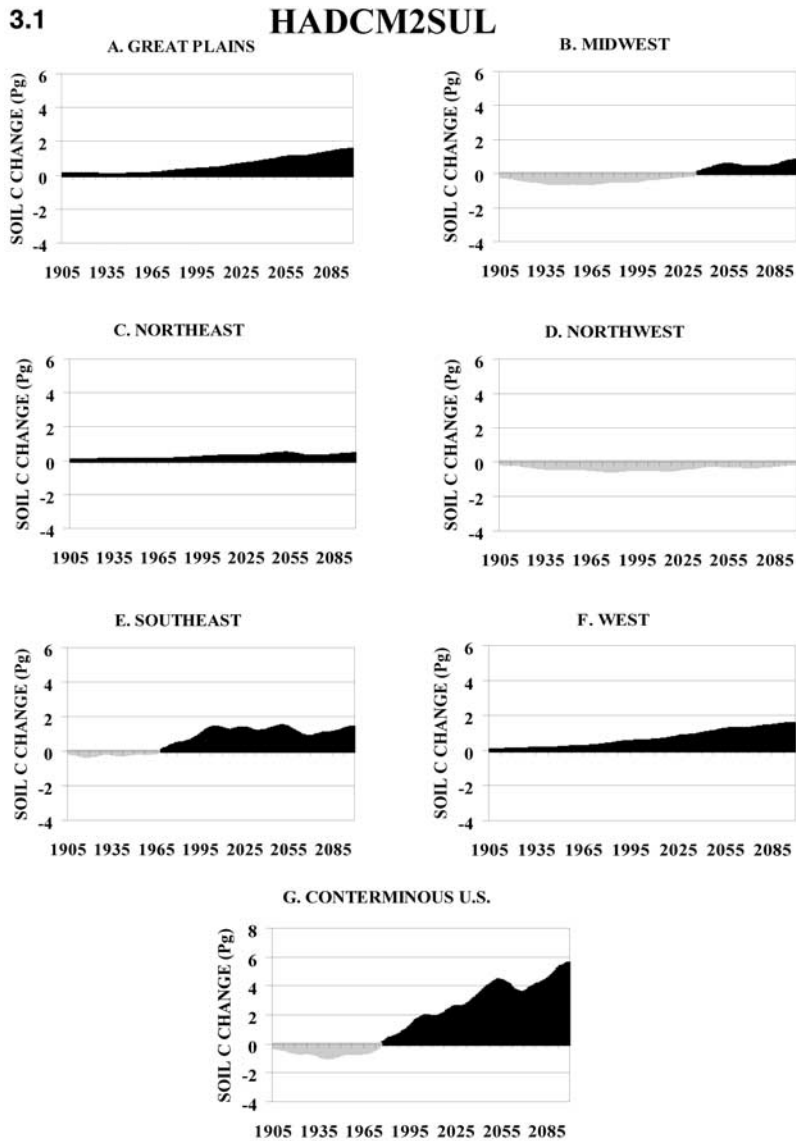


Figure 3. Annual change in soil carbon (10-year average) relative to the 1895 level for the six U.S. GCRP regions as simulated by MC1 from 1895 to 1993 and using (1) HADCM2SUL and (2) CGCM1 future climate change scenarios from 1994 to 2100.

mid-2030s before issuing a dramatic increase up to the end of the century. However, regional differences are pronounced (Figure 4 C and D). The HADCM2SUL scenario is generally wetter across all regions, while the CGCM1 scenario is wetter in the West, the Northwest, and the Midwest, and drier in the Southeast.

A change in the seasonal trend of temperature and precipitation may have as much or more impact on ecosystem properties as changes in annual trends. CGCM1 shows a greater increase than HADCM2SUL in minimum winter temperature by the end of the 21st century in all regions (Figure 5 A and B). Summer precipitation is projected to increase in the Midwest, Southeast, and Northeast regions under HADCM2SUL, whereas it decreases in the Southeast and the Great Plains under CGCM1 (Figure 5 C and D).

Changes in Carbon Pool Sizes from the 1895 Levels with Future Climate Change Scenarios

When one compares the projected size of the total ecosystem carbon pool in the 21st century with the 1895 value, regional differences remain (Figures 2.1 and 2.2). The West and the Great Plains regions continue to show an increase in total carbon from the 1895 level throughout the 21st century under both scenarios (Figures 2.1 A and F, and 2.2 A and F). The model simulates the Midwest region as gaining carbon with regards to the 1895 levels in the 21st century with the HADCM2SUL scenario (Figure 2.1B), while continuing to lose carbon with the warmer CGCM1 scenario (Figure 2.2B). Projections for the Northwest region are the exact opposite, as the region continues to lose carbon

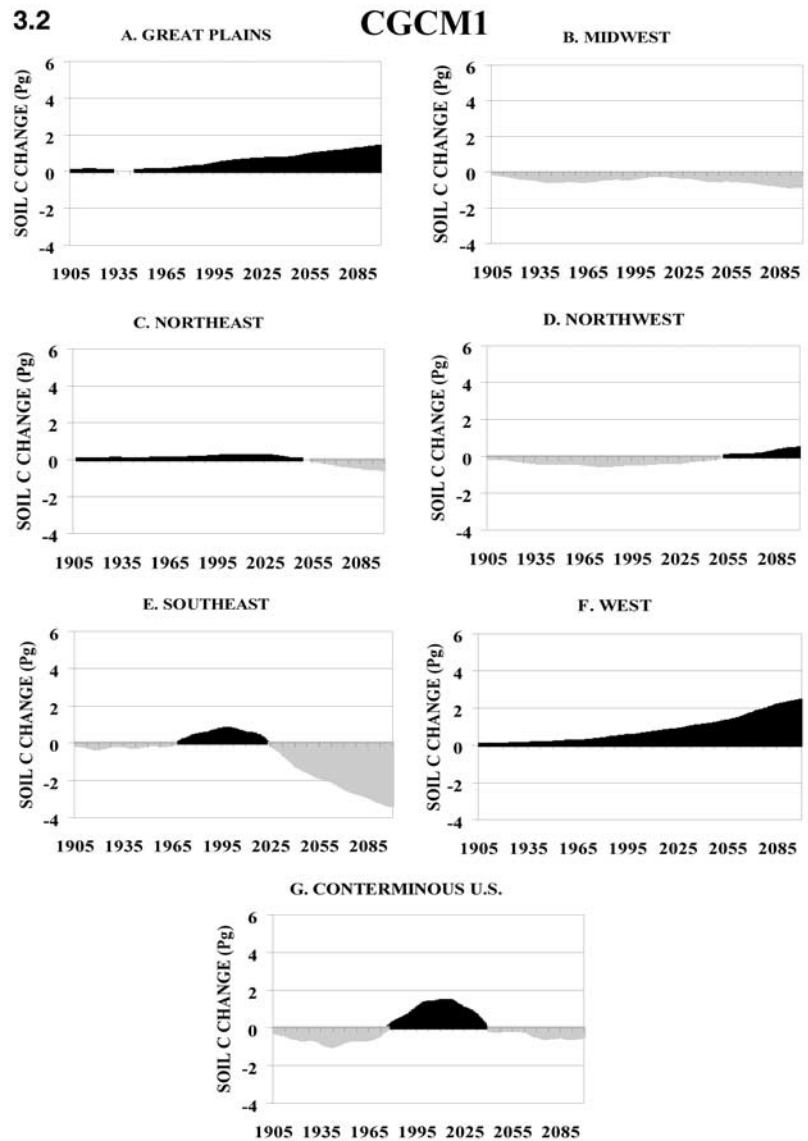


Figure 3. Continued.

with the HADCM2SUL scenario (Figure 2.1D) but starts gaining carbon with regards to the 1895 levels by the end of the 21st century with the regionally wetter CGCM1 scenario (Figure 2.2D). Both the Northeast and Southeast regions switch from carbon gains to carbon losses early in the 21st century under the CGCM1 scenario (Figure 2.2C and E). This does not happen with the milder HADCM2SUL scenario (Figure 2.1C and E). Averaged over the entire country, the total carbon stocks with regards to 1895 levels increase significantly (near 10 Pg C) by the end of the 21st century with the HADCM2SUL scenario, whereas they start decreasing again and showing losses (near -2.5 Pg C) early in the 21st century with the CGCM1 scenario.

Projected changes in soil carbon levels since 1895 follow similar patterns (Figures 3.1 and 3.2). The West and Great Plains regions accumulate carbon from 1895 to the end of the 21st century with both climate scenarios. The Midwest region recovers from losing carbon with regards to 1895 levels with the HADCM2SUL scenario (Figure 3.1B), but not the CGCM1 (Figure 3.2B), whereas the Northwest region gains carbon with CGCM1 (Figure 3.2D). In the Southeast and the Northeast regions, the model simulates losses in soil carbon in the second half of the 21st century with the CGCM1 scenario (Figure 3.2C and E) but not with the milder HADCM2SUL scenario (Figure 3.1C and E). For the country as a whole, soil carbon gains with regards to

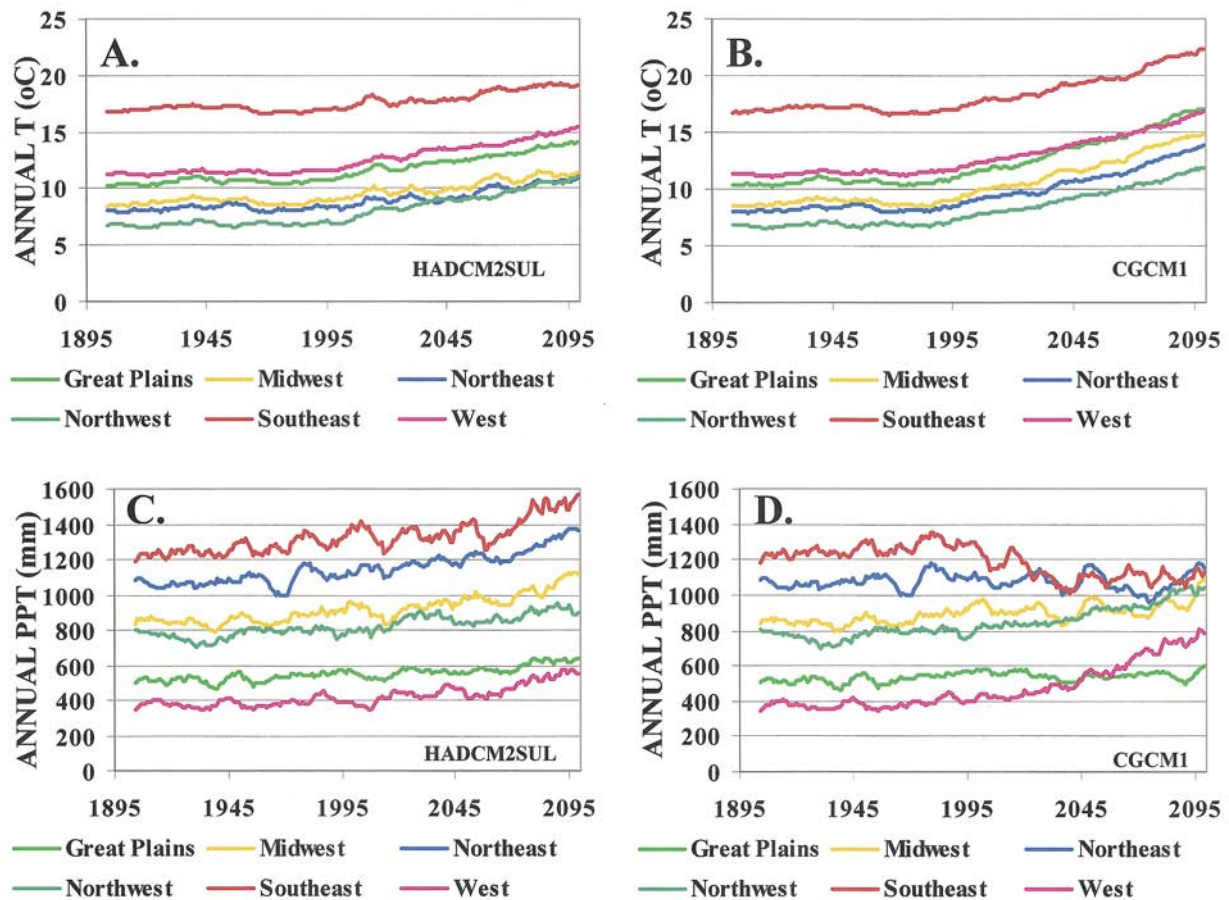


Figure 4. GCM-simulated mean annual temperature and mean annual rainfall (10-year running average between 1895 and 2100) by using HADCM2SUL (A and C) and CGCM1 (B and D) for the six U.S. GCRP regions.

1895 levels increase to near 6 Pg with the HADCM2SUL scenario, whereas they decline and are replaced by losses by mid 21st century with the CGCM1 scenario.

Interannual Changes in Regional Source-Sink Strength

In the **Great Plains** (Figure 6.A), the drought of the 1930s is characterized by a decrease in live plant biomass (up to 50 Tg C y⁻¹) and a small decrease in soil carbon. During the next decade, the region becomes a carbon sink of similar magnitude, with increases in live plant biomass. Smaller decreases in live vegetation biomass occur during the drought of the 1950s and in the 1990s. Because grasslands dominate the Great Plains, the fuel load is large and fires are frequent, with an average biomass of 80 Tg C y⁻¹ consumed in the 20th century. Increases in carbon stocks in the 21st century under CGCM1 correspond mostly to increases in soil carbon except in the 2090s, when increases in live biomass exceed those in soil carbon. Around 2035 and

2085, the biomass consumed by fire increases (125 Tg C y⁻¹), and the region becomes a source of carbon. Both periods correspond to decreases in annual precipitation. Under HADCM2SUL, the region remains a significant carbon sink throughout the century.

The **Midwest** region (which includes the Prairie Peninsula area) is simulated as a source of carbon until the 1940s and at the end of the 20th century (up to 100 Tg C y⁻¹). Increases in live vegetation biomass are simulated (up to 40 Tg C y⁻¹) in the 1920s when they are accompanied by losses in soil carbon, in the early 1940s and in the 1960s (Figure 6.B). Biomass consumption by fire matches the periods when the region is losing carbon. A probable cause is that summer precipitation is on average lower between 1905 and 1940 (274mm) than between 1940 and 1980 (293mm) and shows a decrease from the early 1900s that peaks during the 1930s drought (Figure 5C) and corresponds to a large decrease in both vegetation and soil carbon. In the 21st century under CGCM1, the model simulates this region

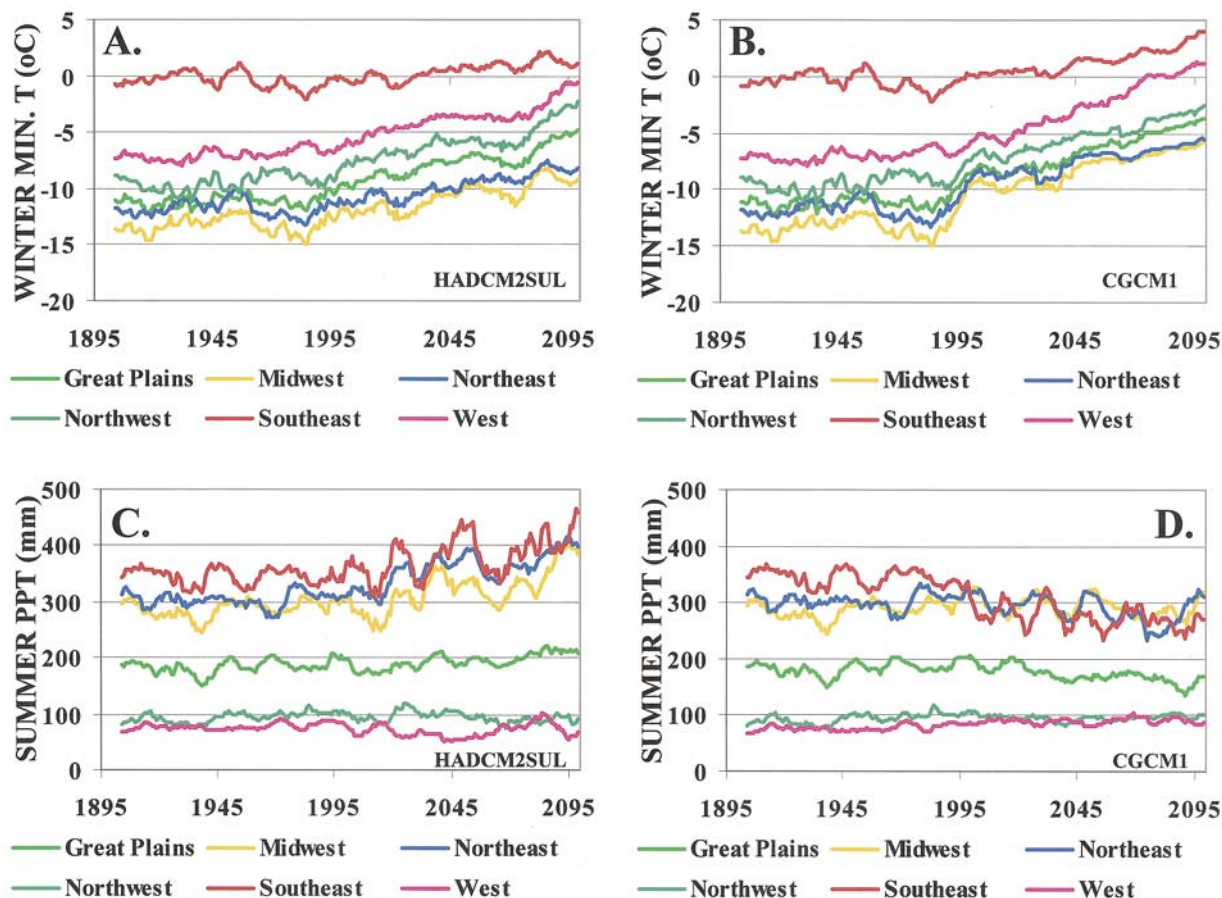


Figure 5. GCM-simulated winter minimum temperature and mean summer rainfall (10-year running average between 1895 and 2100) by using HADCM2SUL (A and C) and CGCM1 (B and D) for the six U.S. GCRP regions.

as alternating between becoming a carbon source (up to 50 Tg C y^{-1}) with significant decreases in soil carbon, or a carbon sink (up to 60 Tg C y^{-1}). Increases in biomass consumed by fire coincide with carbon source strength. Under HADCM2SUL, the region is mostly a carbon sink (up to 80 Tg C y^{-1}) except from the mid-2050s to 2080, when a source is simulated corresponding to higher biomass consumption by fire, probably owing to a decrease in summer precipitation (Figure 5.C).

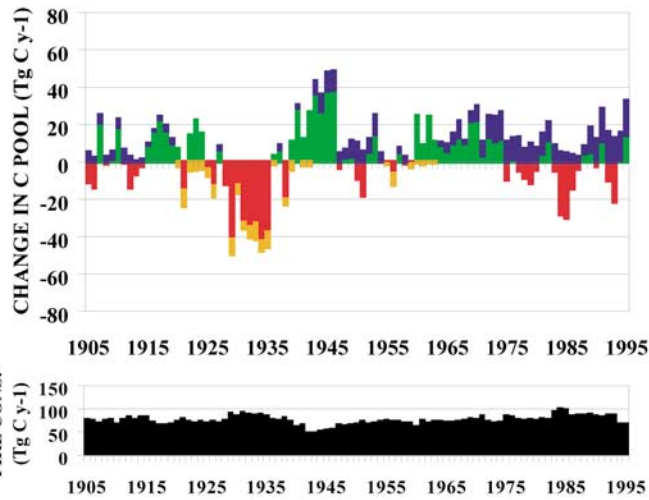
The **Northeast** region (Figure 6.C) is a carbon sink at the end of the historical period. In the 1930s and the 1960s, the region is simulated as a source of carbon corresponding to a few fire events. During the 21st century under CGCM1, the model simulates the region as mostly a source of carbon (up to 50 Tg C y^{-1} in the 2030s) with significant losses in soil carbon in the 2nd half of the century not necessarily matched with fire events. Under HADCM2SUL, the region is simulated as a source of carbon (30 Tg C y^{-1}) for only about 20 years (2050–2070), and as a sink for carbon throughout the

rest of the century with virtually no fires as this scenario simulates milder conditions for the region.

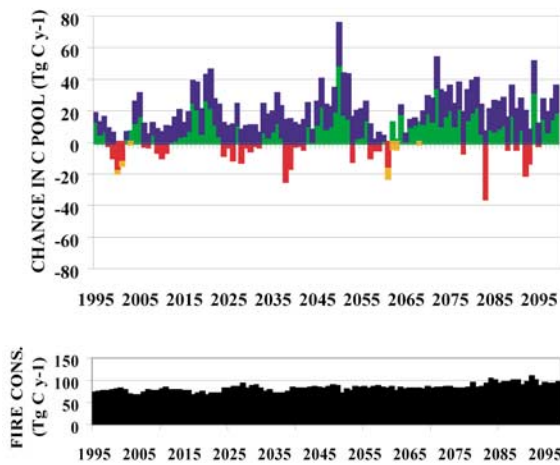
The **Northwest** region is simulated as a source of carbon until the mid-1930s, when for a decade or so its vegetation becomes a sink before the region turns into another carbon source in the 1960s and 70s (Figure 6 D). The 1970s are characterized by a large sink (40 Tg C y^{-1}) in live biomass, followed by increases in soil carbon. During the 21st century under CGCM1, the model simulates mostly a carbon sink potential except in the 2060s. Under HADCM2SUL, the model simulates a greater potential for carbon release throughout the 21st century as temperatures increase, but summer precipitation remains constant throughout the 21st century (Figures 4.A and 5.C). Because much of the region is dominated by grasses and shrubs (interior), the total biomass consumed by fire is large (100 Tg C y^{-1}) and increases towards the end of the 21st century (up to 160 Tg C y^{-1} under CGCM1).

The **Southeast** region is simulated as a sink (up to 100 Tg C y^{-1}) during the historical period and as a

A. GREAT PLAINS



HADCM2SUL



CGCM1

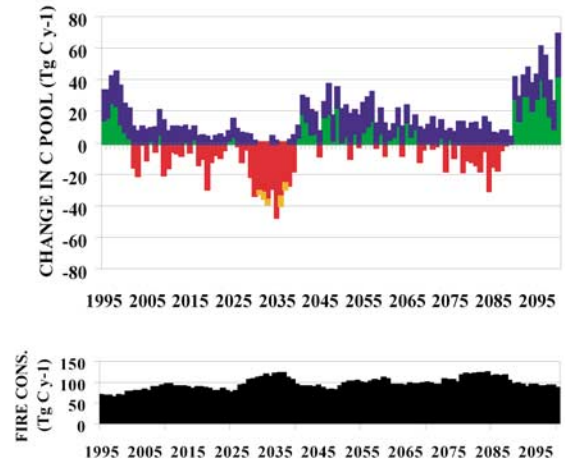


Figure 6. Simulated interannual variation in total ecosystem carbon during the historical period (1895–1993), and under HADCM2SUL and CGCM1 future climate scenarios (10-year running average). Carbon gains in live vegetation (green) and soil (blue), carbon losses from live vegetation (red) and soil (orange), and biomass consumed by fire, for the six U.S. GCRP regions.

large source in the 21st century (250 Tg C y^{-1}) under CGCM1 with an increase in biomass consumed by fire (Figure 6.E). Annual precipitation under CGCM1 drops rapidly by almost 17% in the future projections (Figure 4.D). Under HADCM2SUL, decadal trends in the carbon sequestration potential are clearly visible with the region becoming a source of carbon around 2005, 2025, and 2055. These decadal trends correspond closely with those observed in the 10-year average summer precipitation (Figure 5.C).

The **West** is simulated as a small sink for carbon during the historical period and a larger one during the 21st century under CGCM1 and, to a lesser extent, under HADCM2SUL (Figure 6.F). This is due mostly to increased annual precipitation which doubles under CGCM1 between the beginning and the end of the 21st century (Figure 4.D) while summer precipitation in-

creases only slightly. Winter rains contribute to the replenishment of the soil water resources and allow for tree establishment. The level of biomass consumed by fire is high, since a large fraction of the region is dominated by shrublands and grasslands, which are more prone to fire than forests. Under HADCM2SUL, summer precipitation drops to a low of 54 mm in 2045 (Figure 5.C) before increasing until the end of the century. This decrease in summer precipitation in the first half of the century is probably responsible for the release of carbon as a response to drought stress in the region.

Associated Changes in Vegetation Cover

The spatial distribution and abundance of vegetation are important because vegetation regulates many ecosystem processes and variables, including soil chem-

B. MIDWEST

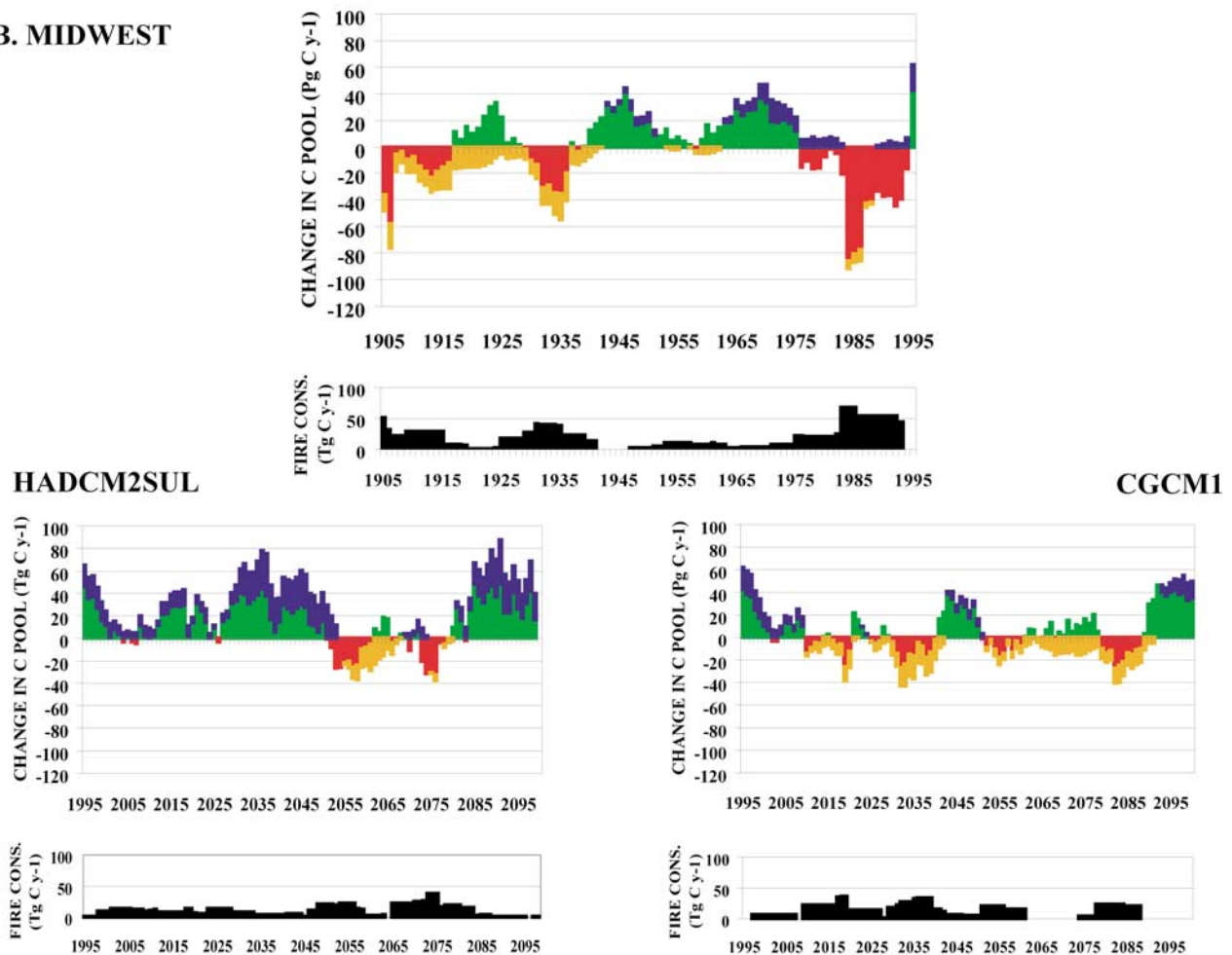


Figure 6. Continued.

istry, water infiltration, water use, soil development, sediment transport, microclimate, wildfire frequency, and food/habitat availability. The forest area is fairly constant throughout the 20th century in most regions except the Midwest, where an increase in total forest area starts in the 1940s and reaches its peak around 1988, when fires in the corn belt or Prairie Peninsula region (not shown) dramatically reduce it (Figure 7.B). In the 21st century, the forested area in the Midwest increases again with both climate change scenarios. However, while the deciduous forests are expanding, the evergreen forests remain low and disappear by 2100 (not shown), as they migrate north into Canada. Both the Northeast and Southeast regions lose a fraction of their forest area (Fig 7C and E) owing to a drought around the 2030–40s simulated under CGCM1 (Figure 4.D) that corresponds to large decreases in total carbon (Figure 6.C and 6.E). The forested area in both the

West and the Northwest regions increases by the end of the century under CGCM1 (Figure 7F and D) owing a large increase in annual rainfall (Figure 4.D), which favors evergreen forests. The forested area in the Great Plains region increases under HADCM2SUL as the eastern deciduous forest expands westward (Fig 7A). This switch to a woodier vegetation cover can explain much of the increase in sink-potential for both the Great Plains and the West (Figure 6.A and 6.F).

Limitations and Uncertainties

Model results depend first on the quality of the climate data that are used. The VEMAP dataset (Kittel and others 2000) provides “the best possible long-term and wall-to-wall representation of historical climate variability and change for use as inputs to ecological model simulation” (Kittel and others 2003). The uncertainty associated with future climate change scenarios has

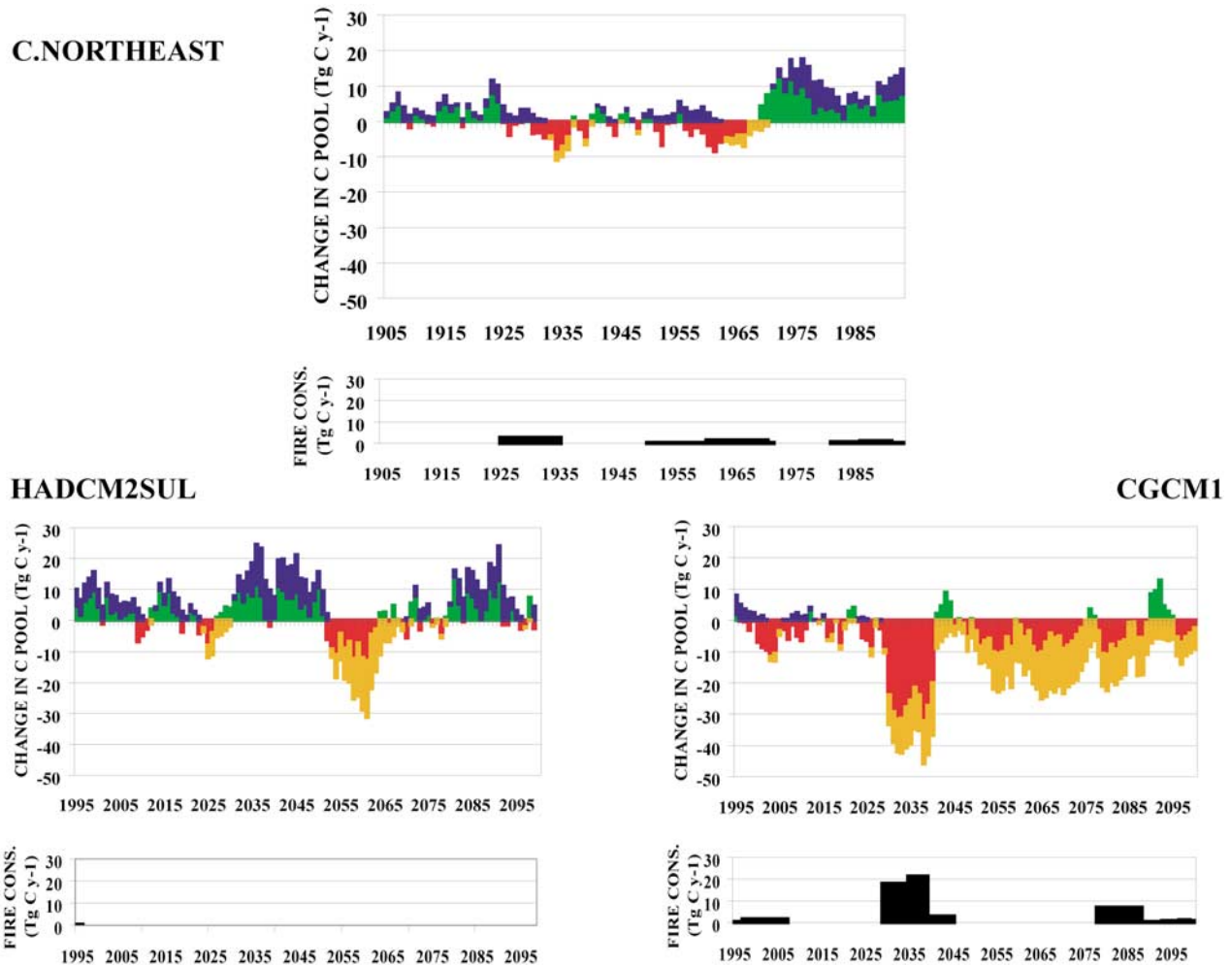


Figure 6. Continued.

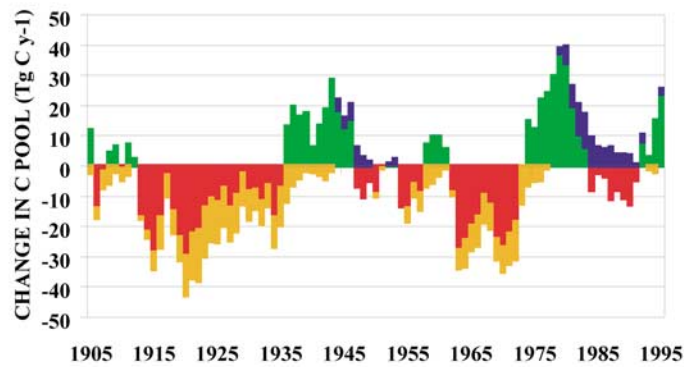
been discussed at length in the appropriate literature and will not be elaborated on here. Our simulations do not include biospheric feedbacks to climate (Bachelet and others 2003).

MC1 simulates potential vegetation and assumes that neither pests nor pathogens affect plant growth, although drought effects, often associated with pests and pathogens, are simulated. No grazing and no human impacts such as agriculture, plantation, pollution, or fire suppression are included in the simulations. Except for droughts and ensuing fires, no extreme events, such as blowdowns, ice storms, or floods, are simulated. It is assumed that all vegetation types are available to grow wherever and whenever the climate permits and that fertile soils are always available. These assumptions were necessitated by the lack of digital gridded time-series of historical management and disturbance patterns at the continental scale as well as a similar lack of

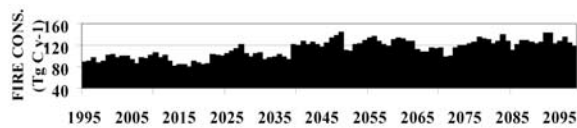
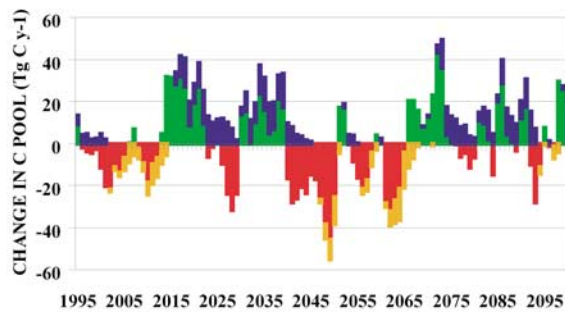
nitrogen and pollution deposition data and natural nitrogen fixation rates. The responses of simulated vegetation to atmospheric CO₂ increases are discussed in detail in Bachelet and others (2003).

MC1 does not simulate fire suppression. It simulates the fraction of a grid cell that is burned by large fires by using biomass and moisture characteristics that are homogeneous in the cell. Observed large wildfires are usually the result of extreme events and depend greatly on local topography. Simulated monthly climate mutes the impact of extreme events of less than a month's duration, and the VEMAP scale is too coarse to represent the complex topography of the western regions. Consequently, the accuracy of fire location and timing in our simulations is limited. It is meant to indicate broad patterns of fire and should not be interpreted as a reliable prediction.

D. NORTHWEST



HADCM2SUL



CGCM1

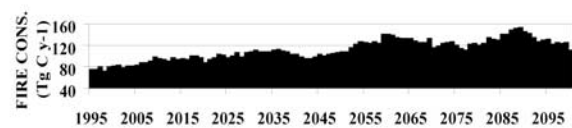
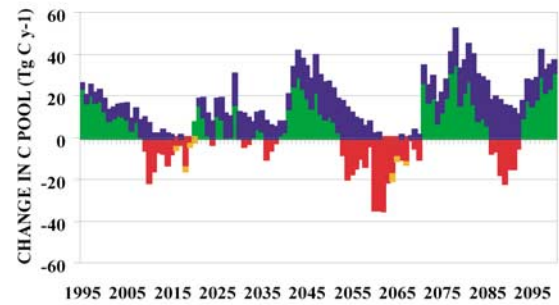


Figure 6. Continued.

Validation efforts have been presented in Bachelet and others (2001 and 2003). Site-level comparisons with eddy-covariance data show reasonable temporal dynamics of net primary production but an overestimation of average NPP owing to the lack of nutrient limitations (unpublished data). Regional results based on observed satellite information (e.g., Hicke and others 2002) are difficult to use for comparison, since they include errors associated with averaging natural and human impacted areas at the regional scale.

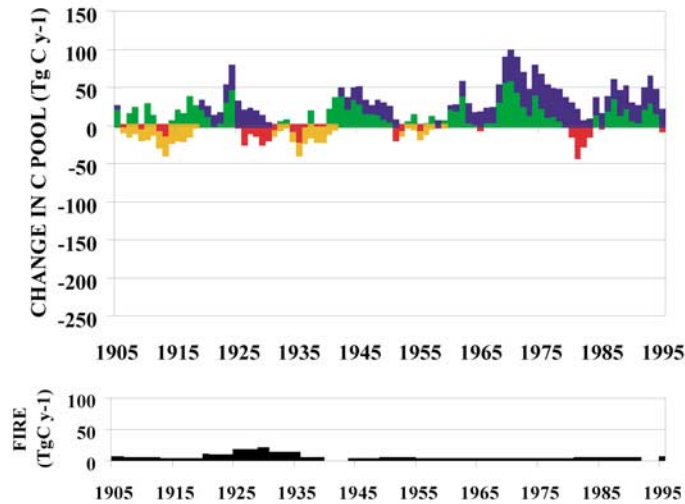
Discussion

Regional simulations illustrate the large spatial variability in the dynamics of the carbon pools in natural vegetation across the conterminous U.S. Most regions (especially in the Great Plains and the Midwest) became a source of carbon during the drought of the

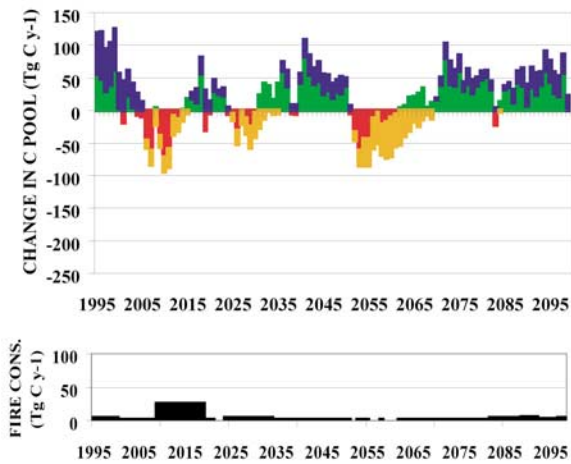
1930s. Simulations also showed that the Northwest (Figure 6.D) was a source of carbon in the 1970s (up to 40 Tg), and during the 1990s (up to 100 Tg). Notably, Midwest and Northwest were the only two regions that lost carbon when 1895 carbon levels are used as a baseline (Figure 2.1B and D). The Southeast became a carbon sink early in the 20th century (Figure 2.1E), but gained soil carbon only after 1970 (Figure 3.1E).

Under future climate change scenarios, MC1 continues to simulate large differences between the various regions. Under the moderate climate scenario (HADCM2SUL), the model shows increasingly large sinks in the Great Plains and the Midwest (at least in the first half of the 21st century). These regions lose carbon under the warmer climate scenario (CGCM1) (Figure 6.A and B). Both scenarios suggest increases in temperature; thus, the differences likely result from a decrease in summer rainfall under CGCM1 (Figure 5.D). Since

E. SOUTHEAST



HADCM2SUL



CGCM1

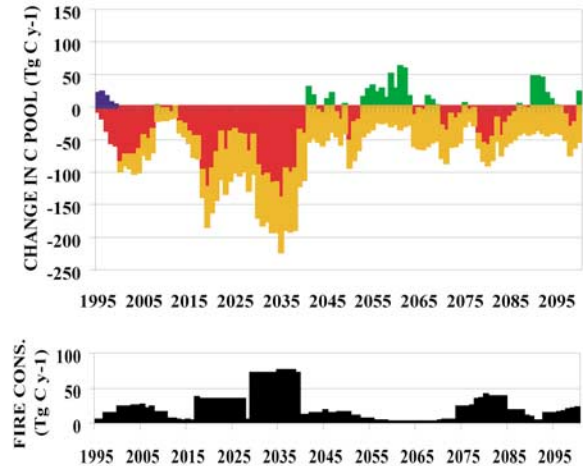


Figure 6. Continued.

the regions are dominated by summer rains, their losses would be significant. Also, under CGCM1, winter temperatures increase in the continental interior, which would result in increased decomposition (Figure 6.B). Under the more extreme CGCM1 scenario, the West (Figure 6.F) is a larger sink for carbon (up to 95 Tg) than under HADCM2SUL. Again, as temperature increases under both scenarios, the difference between them results from larger increases in rainfall under the CGCM1 scenario that compensates for higher evapotranspiration (Figure 5.D). Under CGCM1, both the Northeast and the Southeast become large carbon sources (up to 250 Tg C in the Southeast) during most of the 21st century (Figure 6.C and E) because precipitation decreases (Figures 4.D and 5.D). Under HADCM2SUL, both the Northeast and the Southeast become carbon sources in the 2050s (Figure 6.C and E) because of a large decrease in annual and summer

precipitation (Figures 4.C and 5.C). The Northwest alternates as either a source or a sink of carbon (Figure 6.D) with HADCM2SUL, whereas it is mostly a sink for carbon with CGCM1 except in the 2010s and the 2060s, when up to 40 Tg C are released to the atmosphere. Again, both scenarios show large temperature increases, but precipitation under CGCM1 increases slightly more than under HADCM2SUL.

It is important when we look at the national numbers (Figure 8.B) to also examine the underlying regional patterns (Figure 8.A). While the standard deviation associated with the simulated countrywide net biological production quantifies some of its uncertainty; the underlying contributions of the various regions responsible for this uncertainty become undetectable. For example, the large carbon losses due to wildfires in the Midwest from 1900 to 1940, and in 1988, overcome the gains in other regions and contribute to the coun-

F. WEST

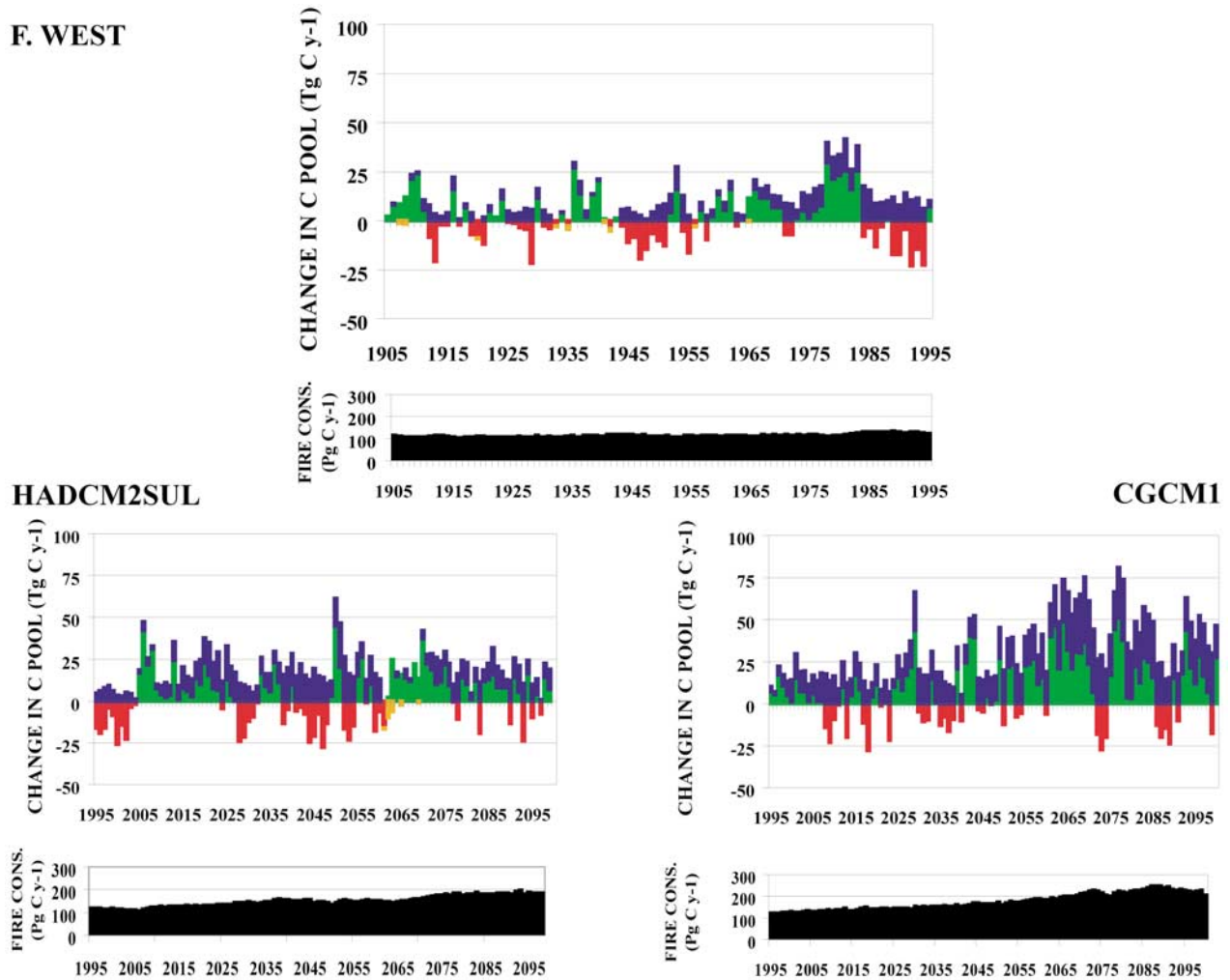


Figure 6. Continued.

trywide signal for these periods as a carbon source. Similarly, carbon losses in the Southeast in the 1950s dominate the signal so that the country is simulated as a carbon source. The size of the sources and sinks is relatively similar between regions (Figure 8.A) with similar standard deviations (about 0.1 Pg, not shown here) except in the Northeast, where the standard deviation values are smaller (0.02 Pg). The largest carbon sources come from the Midwest (15% of the conterminous U.S. area with 57% under agricultural land use), where drought-induced fires reduce both biomass and soil carbon pools. The largest historical carbon sinks ($> 0.05 \text{ Pg y}^{-1}$) are associated with the Great Plains (27% of the conterminous U.S. area with 31% of its area under agricultural land use) and the Southeast (19% of the conterminous U.S. area with 29% under agricultural land use). The Great Plains region is dominated by grasses that are responsible for continuous soil car-

bon sequestration (Figures 3.1A and 3.2A), and the Southeast is dominated by forests thriving under mild climate conditions (Figures 2.E and 3.E). The climate-driven carbon gains in the Plains, Southeast, and even in the Midwest regions from the 1940s through the 1970s undoubtedly contributed significantly to the 'green revolution', which is traditionally attributed entirely to gains in agricultural technology.

From a management point of view, regionally relevant policies will vary greatly across the country. For example in the Northeast (7% of the conterminous U.S. area with 42% under agricultural land use), where the historical carbon sink/source strength is limited (smallest decadal signal in Figure 8.A) and losses to fires are minimal (Figure 9), attention to human impacts such as pollution, nitrogen deposition, urbanization, and other land use changes is more relevant in the short term. Future climatic trends (Figure 6.C) could

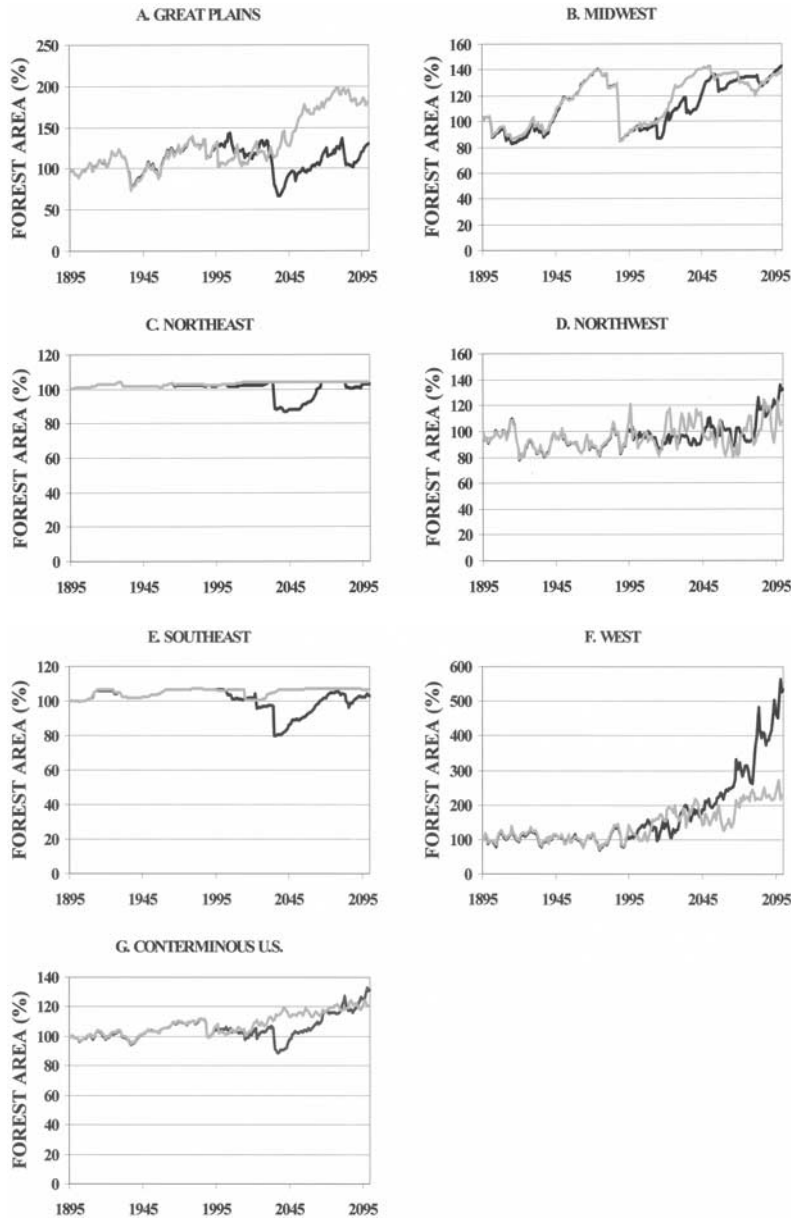


Figure 7. Simulated change in forest area for the 6 U.S. GCRP regions, as a percentage of the total region area in 1895, under historical conditions (1895–1993) and under HADCM2SUL (grey) and CGCM1 (black) future climate scenarios.

increase the impacts of drought on the vegetation and call for more attention given to climatic variability and fire danger. However, the contribution of the natural vegetation to the national carbon budget will remain limited. On the other hand, even though carbon losses due to wildfires are large across the entire western U.S. (Figure 9), fire management will be important in the Midwest where simulated fire-caused carbon losses are the largest (Figure 8.A), albeit fragmented owing to the predominance of agriculture. This region includes the Prairie Peninsula area, which constitutes an ecotone between the eastern deciduous forest and the Plains grasslands, and where climatic variability is large. The

success of carbon sequestration efforts in this region through either maintaining a healthy forest or healthy grasslands accumulating soil carbon will require local managers to deal with the ecotonal climatic variability, which will be greatly affected by future climate.

Regional simulations also illustrate the large temporal variability in the size and sign of the carbon fluxes that ultimately depend on the climate data used as input for the model. In Figure 8.A, three decades stand out when all regions have same-sign carbon fluxes. (1) The period of drought of the 1930s with all negative carbon fluxes was particularly obvious in the Great Plains and the Midwest region (Figures 2.1A, 2.2A,

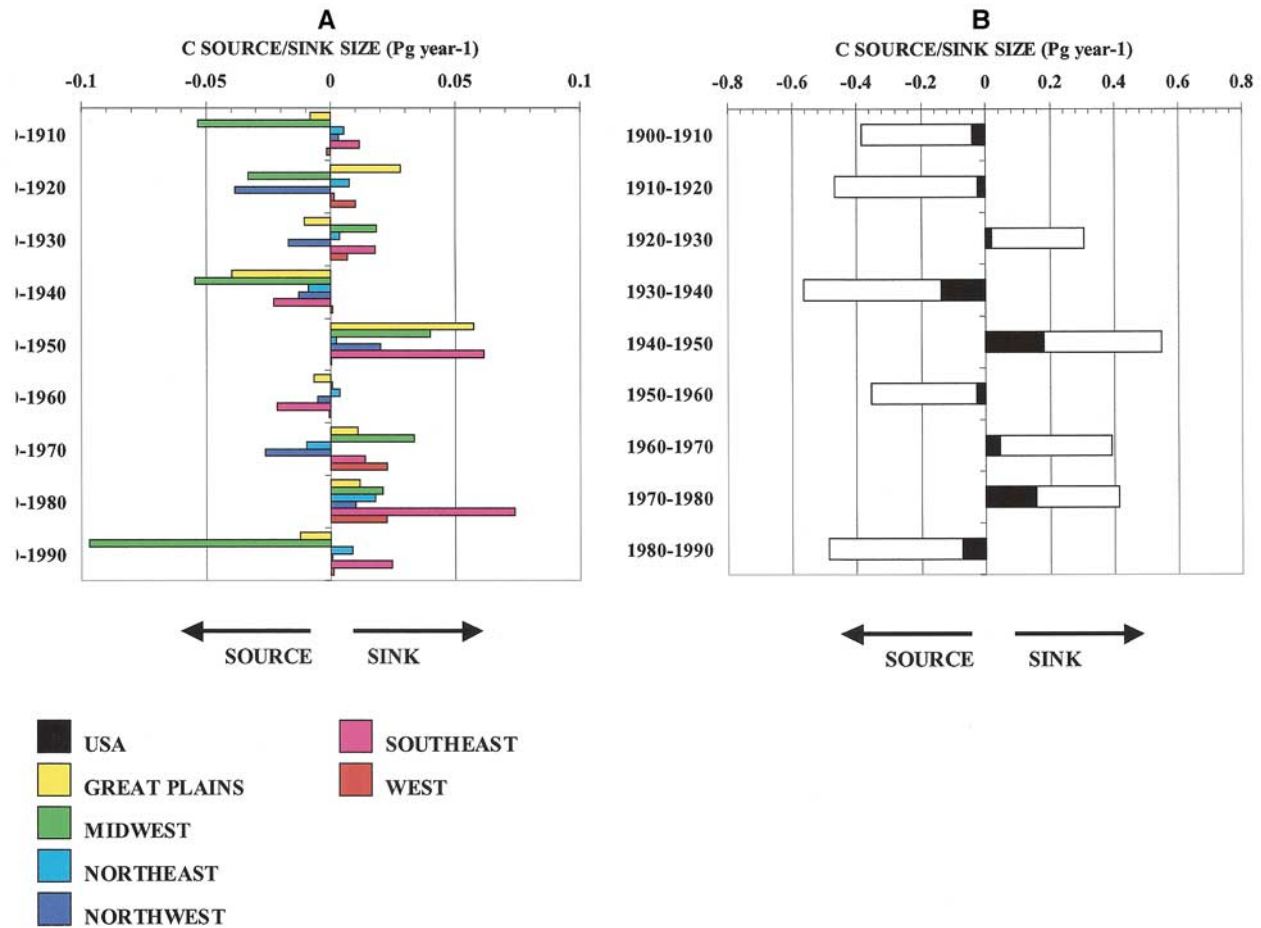


Figure 8. Simulated net biological production decadal averages in Pg C year⁻¹ for (A) the 6 U.S. GCRP regions and (B) the conterminous U.S. with their standard deviation (white) over the 10-year period.

8.A). (2) The recovery and regrowth in the 1940s corresponds to a period of increased precipitation in North America (Karl 1998). (Note that the following drought period of the 1950s had a much smaller effect than that of the 1930s.) (3) The decade of the 1970s, when all carbon fluxes are positive, has been identified as the time of a climate shift (Nicholls and others 1996) and is characterized here by the switch from source to sink in the U.S. total ecosystem carbon budget using the 1895 baseline (Figures 2.1G and 2.2G). This shift was driven by large changes in the Southeast region and in the Northeast and the Northwest, where carbon fluxes all change sign (Figures 6.B, 6.C, 6.D, and 8.A).

Interdecadal climate variability is now being increasingly associated with interdecadal variations in oceanic conditions or oscillations, such as the Pacific Decadal Oscillation (PDO, Mantua and Hare 2002). For example, global temperatures shifted from warming to cooling around 1940–47 and back to warming around 1972–77. These two large-scale atmospheric circulation

shifts correspond to shifts in the PDO and are evident in the regional carbon sequestration patterns revealed by the simulations (Figures 2.1G and 3.1G). The Great Plains, Midwest, Northwest, and Southeast all switched from source to sink (Figure 6.A, B, D, and E) with the PDO shift at about 1940. Although the 1950s drought terminated those gains in the Northwest and Southeast, both regions responded with dramatic carbon gains with the PDO shift in the 1970s (Figure 6D and E), as did the Northeast and the West (Figure 6.C and F). The PDO shift in the 1970s may have initiated a whole new cohort of woody vegetation over much of the interior West and possibly increased the current risk of catastrophic fires in the region (Swetnam and Betancourt 1998). Therefore, the regional responses to the PDO variations appear to have driven a nation-wide shift from carbon source to carbon sink in the 1970s, which would certainly have contributed to the gains determined from direct measurement, but which have been largely attributed to ecosystem responses to past man-

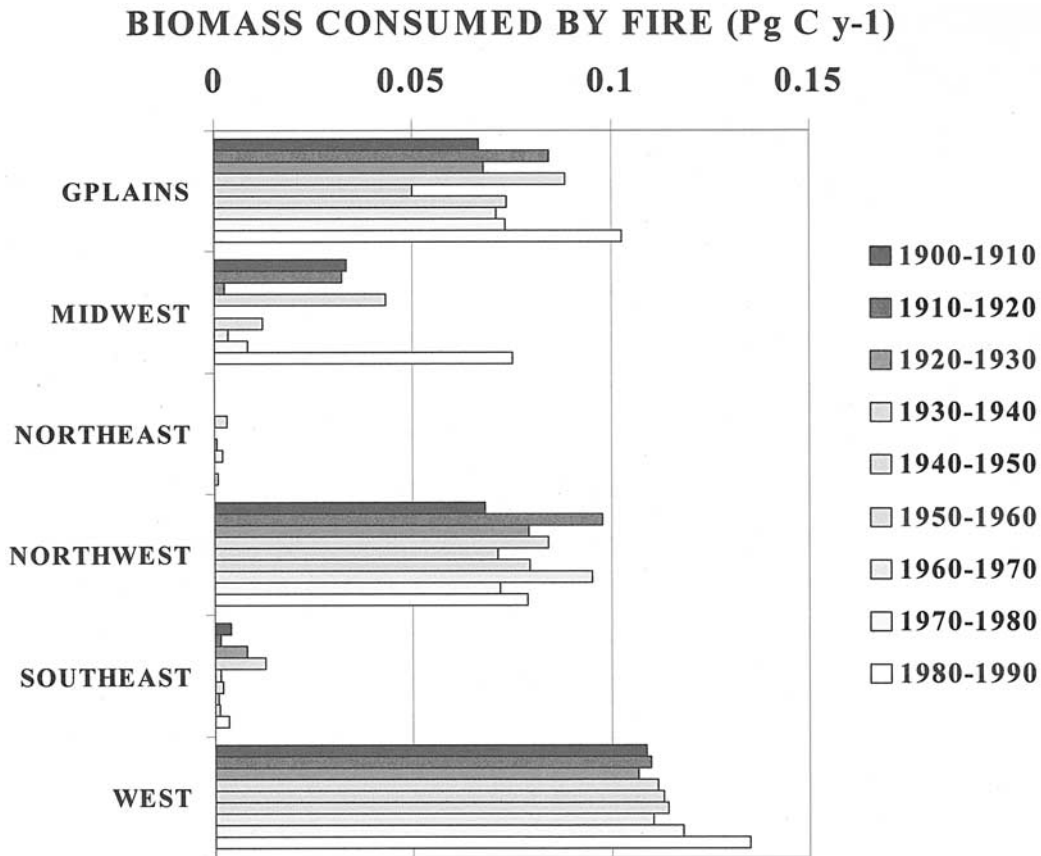


Figure 9. Simulated 10-year average vegetation biomass consumed by wildfires in Pg C year^{-1} for the six U.S. GCRP regions.

agement practices and elevated CO_2 concentrations (Pacala and others 2001).

Pacala and others (2001) calculated that the size of the U.S. carbon sink between 1980 and 1990 varied between 0.26 and 0.43 Pg C y^{-1} owing to changes in forests and non-cropland areas. Our study shows an average value during the 1980s of $-0.074 \text{ Pg C y}^{-1}$ with high regional variation ranging from -0.1 in the Midwest to $+0.025$ in the Southeast for natural vegetation (i.e., not including agricultural lands). The decade of the 1980s is driven in our model simulation by the large simulated wildfires that occurred in the Midwest (Figure 6.B) and the Great Plains. Because of enforced fire suppression since the 1950s that is not simulated in the model, our projections of carbon losses due to fire are overestimated. Moreover, the model simulates vegetation dynamics after fire that include successive replacement of burned forest by grasslands, then woodlands, before canopy closure is simulated (e.g., a decrease in forest area following the simulated 1988 fires; Figure 7.B). Despite this overestimation of fire impacts, MCI simulates the timing and location of catastrophic fires accurately (Lenihan, pers. comm.). In 1988, for exam-

ple, the Yellowstone fires contributed to significant carbon losses in the Great Plains region. It is notable that the Yellowstone fire was accurately simulated even though the model contains no historical fire suppression with attendant fuel buildup, thus indicating a dominant climate forcing of those regional fires.

The fire-induced source of carbon in 1988 is missed by other studies such as Schimel and others. (2000), who used simulation models that either prescribe fires at fixed intervals or include a constant fraction of biomass burned each year. They simulate a carbon sink of $+0.08 \text{ Pg C y}^{-1}$ between 1980 and 1993 by using prescribed fire regimes and also adding to the regional carbon budgets crop yields that are dependent on irrigation and fertilization and only partially on climatic variations.

The discrepancy between our simulation and the published carbon sink strength can thus be explained by our lack of simulation of agricultural areas and of fire suppression. However, we believe that all dryland agriculture and other land-use must survive within environmental constraints and that our model results capture the sensitivity of the natural vegetation in each

region to those constraints. An accurate database of human impacts on the conterminous U.S. is at best scant for the 20th century, and projections of future impacts are only educated guesses, although historical databases are being assembled (Ramankutty and others 2002). Our results pertain directly to the 73% of the conterminous U.S., which is not agricultural, industrial, nor urban, and indirectly to all other areas, given that all areas are subject to climatic constraints. Fire suppression has modified ecosystem responses to climate variability, but most of the observed large wildfires result from extreme events, which are controlled with difficulty. Our model results emphasize the crucial role of the interactions between fire and climate in regulating long-term dynamics in regional carbon fluxes.

Carbon sequestration in ecosystems is an important policy tool for offsetting some carbon emissions from fossil fuel combustion, at least in the short term. However, it will be important to attribute carbon gains or losses in ecosystems directly to human management practices to properly account for fossil fuel offset credits. Our results clearly demonstrate the strong role that climate plays in regional carbon balance and the inherent difficulty in separating the role of human management practices from natural climatic variability. If global warming itself enhances regional and temporal climatic variability (Delworth and others 2002), then identifying the causes of carbon sequestration or loss will be even more difficult.

Acknowledgements

This work was funded in part by the U.S. Department of Energy, National Institute for Global Environmental Change, Great Plains Region (LWT 62-123-06509); the U.S. Geological Survey, Biological Resources Division, Global Change Program (CA-1268-1-9014-10); and the USDA-Forest Service, PNW, NE, SE Stations (PNW 95-0730). The authors thank Tim Kittel and the VEMAP Data group at NCAR (Boulder, CO) for providing us with the climate scenarios. We also thank Steve Wondzell and Cathy Whitlock and two anonymous reviewers for their comments on the paper.

References

- Aber, J., R. Neilson, S. McNulty, J. Lenihan, D. Bachelet, and R. Drapek. 2001. Forest processes and global environmental change: predicting the effects of individual and multiple stressors. *Bioscience* 51:735–751.
- Bachelet, D., J. Lenihan, C. Daly, and R. Neilson. 2000. Interactions between fire, grazing and climate change at Wind Cave National Park, SD. *Ecological Modelling* 134:229–224.
- Bachelet, D., Lenihan, J., Daly, C., Neilson, R., Ojima, D., Parton, W. (2001a) MCI: a dynamic vegetation model for estimating the distribution of vegetation and associated ecosystem fluxes of carbon, nutrients, and water. U.S.D.A. Forest Service, Pacific Northwest Station. General Technical Report PNW-GTR-508.
- Bachelet, D., R. P. Neilson, J. M. Lenihan, and R. J. Drapek. 2001b. Climate change effects on vegetation distribution and carbon budget in the U.S. *Ecosystems* 4:164–185.
- Bachelet, D., R. P. Neilson, T. Hickler, R. J. Drapek, J. M. Lenihan, M. T. Sykes, B. Smith, S. Sitch, and K. Thonicke. 2003. Simulating past and future dynamics of natural ecosystems in the United States. *Global Biogeochemical Cycles* 17:1045, doi:10.1029/2001GB001508.
- Birdsey, R.A., Heath, L.S. (1995) "Carbon changes in U.S. Forests." In: Joyce, L.A. (Eds), *Productivity of America's forests and climate change*, USDA-FS GTR RM-271, pp 56–70.
- Birdsey, R. A., A. J. Plantinga, and L. S. Heath. 1993. Past and prospective carbon storage in United States forests. *Forest Ecology and Management* 58:33–40.
- Bousquet, P., P. Peylin, P. Ciais, C. Le Quere, P. Friedlingstein, and P. P. Tans. 2000. Regional changes in carbon dioxide fluxes of land and oceans since 1980. *Science* 290:1342–1346.
- Brown, S. L., and P. E. Schroeder. 1999. Spatial patterns of aboveground production and mortality of woody biomass for eastern U.S. Forests. *Ecological Applications* 9:968–980.
- Daly, C., D. Bachelet, J. M. Lenihan, R. P. Neilson, W. Parton, and D. Ojima. 2000. Dynamic simulation of tree-grass interactions for global change studies. *Ecological Applications* 10:449–469.
- Delworth, T. L., R. J. Stouffer, K. W. Dixon, M. J. Spelman, T. R. Knutson, A. J. Broccoli, P. J. Kushner, and R. T. Wetherald. 2002. Review of simulations of climate variability and change with the GFDL R30 coupled climate model. *Climate Dynamics* 19:555–574.
- Easterling, D. R., G. A. Meehl, C. Parmesan, S. A. Changnon, T. R. Karl, and L. O. Mearns. 2000. Climate extremes: observations, modeling, and impacts. *Science* 289:2068–2074.
- Falkowski, P., R. J. Scholes, E. Boyle, J. Candell, D. Canfield, J. Elser, N. Gruber, K. Hibbard, P. Hogberg, S. Linder, F. T. Mackenzie, B. Moore III, T. Pedersen, Y. Rosenthal, S. Seitzinger, V. Smetacek, and W. Steffen. 2000. The global carbon cycle: a test of our knowledge of earth as a system. *Science* 290:291–296.
- Fan, S., M. Gloor, J. Mahlman, S. Pacala, J. Sarmiento, T. Takahashi, and P. Tans. 1998. A large terrestrial carbon sink in North America implied by atmospheric and oceanic carbon dioxide data and models. *Science* 282:442–446.
- Hicke, J. A., G. P. Asner, J. T. Randerson, C. Tucker, S. Los, R. Birdsey, J. C. Jenkins, C. Field, and E. Holland. 2002. Satellite-derived increases in net primary productivity across North America, 1982–1998. *Geophysical Research Letters* 29:10, 10.1029/2001GL013578.
- Houghton, R., and J. Hackler. 2000. Changes in terrestrial carbon storage in the United States. 1: The roles of agriculture and forestry. *Global Ecology and Biogeography* 9:125–144.
- Houghton, R. A., J. L. Hacker, and K. T. Lawrence. 1999. The

- U.S. Carbon Budget: contributions from land-use change. *Science* 285:574–578.
- Karl, T. R. 1998. Regional trends and variations of temperature and precipitation. . Pages 412–425 in R. T. Watson, M. C. Zinyowera, R. H. Moss, and D. J. Dokken. Eds, *The regional impacts of climate change: an assessment of vulnerability*. Cambridge University Press, Cambridge.
- Kattenberg, A., F. Giorgi, H. Grassl, G. Meehl, J. Mitchell, R. Stouffer, T. Tokioka, A. Weaver, and T. Wigley. 1996. Climate models: projections of future climate. Pages 285–357 in J. Houghton, L. Meira Filho, B. Callander, N. Harris, A. Kattenberg, and K. Maskell. Eds, *Climate change 1995: the science of climate change. Contribution to Working Group 1 to the Second Assessment Report of the Intergovernmental Panel on Climate*. Cambridge University Press, Cambridge, U.K.
- Keane, R., C. Hardy, and K Ryan. 1997. Simulating effects of fire on gaseous emissions and atmospheric carbon fluxes from coniferous forest landscapes. *World Resource Review* 9:177–205.
- Keeling, C. D., Bacastow, R. B., Carter, A. F., Piper, S. C., Whorf, T. P., Heimann, M., Mook, W. G., Roeloffzen, H. 1989. A three-dimensional model of atmospheric CO₂ transport based on observed winds: 1. Analysis of observational data, in D.H. Peterson (ed.) *Aspects of climate variability in the Pacific and the Western Americas. Geophysical Monographs* 55:165–236.
- Kittel, T. G. F., Rosenbloom, N. A., Kaufman, C, Royle, J. A., Daly, C., Fisher, H. H., Gibson, W. P., Aulenbach, S., McKeown, R., Schimel, D. S., VEMAP2 Participants. 2000. VEMAP Phase 2 Historical and Future Scenario Climate Database, available on line at <http://www.cgd.ucar.edu/vemap> for the VEMAP Data Group, National Center for Atmospheric Research, Boulder, Colorado.
- Kittel, T. G. F., Rosenbloom, N. A., Royle, A., Daly, C., Gibson, W. P., Fisher, H. H., Thornton, P., Yates, D. N., Aulenbach, S., Kaufman, C., McKeown, R., Bachelet, D., Schimel, D.S, VEMAP2 Participants. The VEMAP phase 2 bioclimatic database. I. A gridded historical (20th century) climate dataset for modeling ecosystem dynamics across the conterminous United States. Submitted to *Climate Research* 2003.
- Lenihan, J. M., C. Daly, D. Bachelet, and R. P. Neilson. 1997. Simulating broad-scale fire severity in a dynamic global vegetation model. *Northwest Science* 72:91–103.
- Mantua, N. J., and S. R. Hare. 2002. The Pacific decadal oscillation. *Journal of Oceanography* 58:35–44.
- NAST (National Assessment Synthesis Team) (2000) *Climate change impacts on the United States. The potential consequences of climate variability and change*. Available at: <http://www.usgcrp.gov/usgcrp/nacc/default.htm>, and Cambridge University Press
- Neilson, R 1995. A model for predicting continental-scale vegetation distribution and water balance. *Ecological Applications* 5:362–385.
- Nicholls, N, G. V. Gruza, J. Jouzel, T. R. Karl, L. A. Ogallo, and D. E. Parker. 1996. . Pages 133–192 in J. T. Houghton, L. G. Meira Filho, B. A. Callander, N. Harris, A. Kattenberg, and K. Maskell. Eds, *Climate change 1995: the science of climate change. Contribution of Working Group 1 to the Second Assessment Report of the Intergovernmental Panel of Climate Change*. Cambridge University Press, Cambridge, UK.
- Pacala, S. W., G. C. Hurtt, D. Baker, P. Peylin, R. A. Houghton, R. A. Birdsey, L. Heath, E. T. Sundquist, R. F. Stallard, P. Ciais, P. Moorcroft, J. P. Caspersen, E. Shevliakova, B. Moore, G. Kohlmaier, E. Holland, M. Gloor, M. E. Harmon, S. -M. Fan, J. L. Sarmiento, C. L. Goodale, D. Schimel, and C. B. Field. 2001. Consistent land- and atmosphere-based U.S. carbon sink estimates. *Science* 292:2316–2320.
- Parton, W. J., D. S. Schimel, C. V. Cole, and D. Ojima. 1987. Analysis of factors controlling soil organic levels of grasslands in the Great Plains. *Soil Science Society of America* 51:1173–1179.
- Parton, W., Schimel, D. Ojima, D., Cole, C. 1994. A general study model for soil organic model dynamics, sensitivity to litter chemistry, texture, and management. Pages 147–167 in *Soil Science Society of America Special Publication* 39
- Peterson, D., and K. Ryan. 1986. Modeling postfire conifer mortality for long-range planning. *Environmental Management* 10:797–808.
- Potter, C. S., and S. A. Klooster. 1999. Detecting a terrestrial biosphere sink for carbon dioxide: interannual ecosystem modeling for the mid-1980s. *Climatic Change* 42:489–503.
- Ramankutty, N., J. A. Foley, J. Norman, and K. McSweeney. 2002. The global distribution of cultivable lands: current patterns and sensitivity to possible climate change. *Global Ecology and Biogeography* 11:377–392.
- Rothermel, R. 1972. A mathematical model for fire spread predictions in wildland fuels. USDA Forest Service Research Paper INT-115, 40 pp.
- Schimel, D., J. Melillo, H. Tian, A. D. McGuire, D. Kicklighter, T. Kittel, N. Rosenbloom, S. Running, P. Thornton, D. Ojima, W. Parton, R. Kelly, M. Sykes, R. Neilson, and B. Rizzo. 2000. Contribution of increasing CO₂ and climate to carbon storage by ecosystems in the United States. *Science* 287:2004–2006.
- Strauss, D., L. Bednar, and R. Mess. 1989. Do one percent of forest fires cause ninety-nine percent of the damage?. *Forest Science* 35:319–328.
- Swetnam, T. W., and J. L. Betancourt. 1998. Mesoscale disturbance and ecological response to decadal climatic variability in the American Southwest. *Journal of Climate* 11:3218–3147.
- Turner, D. P., G. J. Koerper, M. E. Harmon, and J. Lee. 1995. A carbon budget for forests of the conterminous United States. *Ecological Applications* 5:421–436.
- Turner, M., and W. Romme. 1994. Landscape dynamics in crown fire ecosystems. *Landscape Ecology* 9:59–77.
- van Wagner, C. E. 1993. Prediction of crown fire behavior in two stands of jack pine. *Canadian Journal of Forest Research* 23:442–449.